Simulation as a Tool for Evaluating Biogas Purification Processes

Markku Ohenoja[1] Aki Sorsa[1]

[1]Control Engineering, Department of Technology, University of Oulu, Finland, forename.lastname@oulu.fi

Abstract

Biogas is an interesting fuel for the decentralized energy production as it can originate from many different sources. The purification of biogas to the point where it can also be used as a substitute for natural gas requires several purification steps. This paper focuses on the separation of carbon dioxide. A common solver using the discretized Gauss-Seidel method was applied for three different biogas purification process models describing MEA absorption, pressurized water scrubbing and multistage membrane separation. Simulations based on experimental designs were conducted in order to evaluate the applicability of those purification processes for different sources of biogas. The models used were rather simplified descriptions of the processes aimed to describe the directions of the changes in a general manner and to indicate the controllability of the processes.

Keywords: CO_2 separation, Steady-state mass balance, Discretized Gauss-Seidel method, Full factorial design

1 Introduction

The search for more efficient and environmentally friendly energy sources is a continuously treated topic in politics, marketing, business and, of course, in science. It is naive to expect that science finds one groundbreaking technique to decrease the dependency on fossil fuels. More probably a large number of feasible solutions for clean and efficient energy production will be used in parallel. This means that there would be a growing interest also on energy production in different scales. Biogas (biomethane) is a particularly interesting option: It can be collected as a landfill gas or be produced by anaerobic digestion from many different feed stocks regarded as a waste material, such as wastewater sludge, industrial by-products, manure and food residue. Biogas production is sizable and the product is storable and therefore it can be produced in various different locations and in many different scales. It also has a high number of possible end-users as it is suitable for transport fuel, heat production and combined heat and power production. Potentially, 50% of the present natural gas consumption in the EU could be replaced by biogas within the five next years (Wellinger et al. 2013).

The composition of biogas varies according to its source. It includes impurities among methane and thus purification is needed in order to use biogas as a substitute for natural gas. The efficiency of this upgrading is significant to gain environmental benefits compared with fossil fuels. The purified biogas must have high enough methane content while the energy consumption must stay at low enough levels. This is a challenging task not only because of the number of impurities present but also because of the changes in inlet biogas composition. Furthermore, the planned way of usage may set tight requirements for the produced biogas.

Biogas purification may require a separation of large number of impurities including e.g. carbon dioxide, nitrogen, oxygen, hydrogen sulphide, ammonia and siloxanes (Wellinger et al. 2013). The purification process should therefore require a combination of methods such as absorption, adsorption, molecular sieves, membrane separation, condensation, cryogenics or ultrasonic separation. The purification steps needed depend on the composition of the inlet biogas and must be able to satisfy the criteria set for the produced gas. Designing such a purification scheme is a complex task where simulation offers valuable tools for evaluating and comparing different alternatives. However, the simulators must give realistic results and must be able to evaluate process performance and energy consumption in order to gain knowledge of proper processing schemes.

This paper concentrates on CO_2 separation where pressurized water scrubbing, chemical absorption, membrane separation and pressure swing adsorption are currently the most economically feasible methods. Mechanistic models of the three first purification processes are given in this paper. Also the energy consumption is approximated. Simulations using the discretized Gauss-Seidel solver are carried out with the models in order to evaluate their applicability for different sources of biogas. Through simulations, the sensitivity of the processes is evaluated to gain knowledge of the effects of certain disturbance and design variables on energy consumption and process behavior. The models used are rather simplified descriptions of the processes as they are expected to give the directions of the changes in a general manner and indicate the controllability of the processes. More detailed models are presented in literature. For example, (Scholz 2013) presents a membrane model incorporating a number of non-ideal effects and (Kucka et al. 2003) provide a rigorous rate-based model for

carbon capture with chemical absorption including tens of thousands of equations.

2 Modeling

Three processes for CO_2 bulk separation from biogas are considered: pressurized water scrubbing, chemical absorption with monoethanolamine (MEA) and membrane separation. The two former ones rely on the same model structure.

2.1 Absorption model

The absorption model incorporates the steady-state mass balance equations for the gas and liquid phase components that have a gradient along the absorption column height. In the gas phase, the mass transfer is negative as material is absorbed into the liquid phase. In liquid phase, there can be positive mass transfer due to absorption but also loss of material due to chemical reaction. The absorption rate $N_i, [mol/m^3 \cdot s]$ for component i can be written as:

$$N_i = K_i\left(C_{L,i}^{if} - C_{L,i}^{bulk}\right) \tag{1}$$

where K_i is the overall volumetric mass transfer coefficient $(1/s)$, $C_{L,i}^{if}$ is the concentration (mol/m^3) of component i at the vapor-liquid equilibrium (VLE) and $C_{L,i}^{bulk}$ is the concentration of component i at the bulk liquid. The equilibrium state (interface concentration) is approximated using Henry's law:

$$p_{G,i}^{if} = p_{G,i}^{bulk} = H_i C_{L,i}^{if} \tag{2}$$

where H_i is the Henry's law coefficient $(Pa \cdot m^3/mol)$. The coefficients were taken from Greer (2008) and Mohebbi et al. (2012):

$$\begin{aligned} H_{CO2}^{MEA} &= x_{MEA} exp(170.7126 \\ &\quad - 8477.771/T_L \\ &\quad - 21.95743 log(T_L) \\ &\quad + 0.005781 T_L) \\ H_{CO2}^{H2O} &= x_{H2O} exp(89.452 - 2934.6/T_L \\ &\quad - 11.592 log(T_L) \\ &\quad + 0.01644 T_L) \\ H_{CH4}^{H2O} &= exp\big(-7.037 + 0.1017 T_L \\ &\quad - 0.0001426 {T_L}^2 \\ &\quad + 100P/(83.15 T_L)\big) \end{aligned} \tag{3}$$

The above-mentioned coefficients need to be divided by the total liquid concentration in order to get the SI-units $Pa \cdot m^3/mol$ used in the model above-mentioned.

The overall volumetric mass transfer coefficient is an experimental constant that is related to the individual film mass transfer coefficients in the gas phase and liquid phase and the gas-liquid effective interfacial area. Here it is assumed that the overall mass transfer coefficient incorporates the specific interfacial area and that the coefficient is given in the form applicable to the concentration gradient. The chemical reaction has a positive effect on mass transfer and an enhancement factor E is introduced to the mass transfer coefficient. The enhancement factor is the ratio between the mass transfer coefficient for chemical absorption and the mass transfer coefficient of physical absorption. The calculation of the enhancement factor requires the knowledge of chemical properties such as diffusivity and is also affected by the chemical reaction kinetics. In our case, the enhancement factor is assumed pre-known and constant throughout the column. The relationship between the enhancement factor and the mass transfer coefficients is given by:

$$K_{i,chemical} = E \cdot K_{i,physical} \tag{4}$$

It is assumed that the liquid phase is dilute i.e. no significant change in total liquid flow rate in the column take place. Also the inert gas molar flow rates are naturally constant. It is further assumed that all of the absorbed amount of component i reacts immediately in the chemical absorption. Therefore no accumulation occurs in the liquid phase for that component, i.e. $C_{L,i}^{bulk}$ is zero in chemical absorption. The balance equations in terms of molar flows (mol/s) for component i in gas phase $n_{G,i}$ and liquid phase $n_{L,i}$ can now be written as:

$$\begin{aligned} \frac{1}{A_c}\frac{dn_{G,i}}{dz} &= -N_i \\ \frac{1}{A_c}\frac{dn_{L,i}}{dz} &= \alpha_{ji} N_i \end{aligned} \tag{5}$$

where A_c is the cross-sectional area of the column, α is the stoichiometric factor of the reaction in chemical absorption and z is the distance from the bottom of the column.

2.2 Membrane model

The gas separation membrane model consists of steady-state mass balance equations for the retentate (feed) and permeate sides. The mass transfer is described with the solution-diffusion model. It is assumed that the system is isothermic and there is no pressure gradient along the membrane length. It is further assumed that there are no interactions between the permeance of different components in the system. The molar flux through the membrane $N_i, [mol/m^2 \cdot s]$can be described as:

$$N_i = Q_i\left(p_{R,i} - p_{P,i}\right) \tag{6}$$

where $Q_i, [mol/m^2 \cdot h \cdot bar]$ is the permeance of component i and $p_{R,i}$ and $p_{P,i}$ are the partial pressures of component i in the retentate side and permeate side, respectively. The mass transfer exchange area A in the membrane is equal to the surface area of the membrane multiplied by the number of fibers nof in the membrane system given by:

$$A = nof \cdot 2\pi r \cdot L = nof \cdot \pi d \cdot L \tag{7}$$

where r and d are the radius and the diameter of a single fiber and L is the length of the fiber. The discretized mass balance in terms of molar flows of component i in the retentate and permeate side can be written as:

DOI 10.3384/ecp1511955

$$\frac{dn_{R,i}}{dz} = -N_i A = nof \cdot Q_i\left(p_{P,i} - p_{R,i}\right) \cdot \pi d$$
$$\frac{dn_{P,i}}{dz} = N_i A = nof \cdot Q_i\left(p_{R,i} - p_{P,i}\right) \cdot \pi d \quad (8)$$

The membrane is assumed to be operated in counter-current mode that usually is preferred as it increases the driving force. The model uses the permeance values given in $mol/m^2 \cdot h \cdot bar$. However, the permeances are often given in different units, such as GPU or $m^3/m^2 \cdot h \cdot bar$. Therefore, the following equations need to be applied:

$$Q_i[m^3_{STP}/m^2 \cdot h \cdot bar] = 2.7 \cdot 10^{-3} Q_i[GPU]$$
$$Q_i[mol/m^2 \cdot h \cdot bar] = \frac{P_{STP}}{T_{STP}R} Q_i[m^3_{STP}/m^2 \cdot h \cdot bar] \quad (9)$$

where $P_{STP} = 1 \cdot 10^5 Pa$, $T_{STP} = 273.15\ K$ and $R = 8.314\ Pa \cdot m^3/mol \cdot K$.

The multistage membrane system modelled has two stages with permeate recycling from the second membrane stage to the feed. First, the second membrane molar flows are solved and the results are iterated until they meet the molar flows leaving the first membrane.

2.3 Numerical algorithm

The discretized model equations were solved with a finite difference Gauss-Seidel method (Makaruk & Harasek, 2009). In this method, the half-step and full-step operations are calculated for each discrete point and the gradients are extrapolated using a relaxation factor. The results are then iterated until a pre-defined convergence criterion is fulfilled (or maximum number of iterations are performed). Hence the numerical algorithm has three adjustable parameters: the number of discrete elements, a relaxation factor and a convergence criterion.

2.4 Energy requirement calculations

In order to estimate the energy consumption of the modelled separation processes, models for the energy consumption of a compressor, a pump and a reboiler are presented. The energy consumption of water scrubbing is dependent on the amount of washing liquid pumped, whereas the energy consumption of chemical absorption mainly depends on the reboiler duty required in the regeneration stage. The energy consumption of membrane process is related to the operation pressure of the system. In all processes, additional compression may be required to bring the purified gas to pre-required system pressure.

The compressor model uses the compressor shaft power equation given in (Hall 2012). A motor efficiency of 0.75 is assumed. The pump model is the equation used for the recirculation pump of an absorption column in (Scholz 2013). The simulations assume an overall efficiency of 0.75. The reboiler model adopted from (Scholz 2013) assumes that the heat duty is proportional to the mass flow of absorbed component entering the desorption stage and the heat of reverse reaction between the absorbed component and MEA. The molar flow of MEA was estimated from the consumption of MEA in the process.

2.5 Model validation

The models were validated against several literature results. The validation results, however, are not presented here in detail due to limited space.

The membrane model was validated against a two-component system described in (Scholz 2013), a three-component system presented in (Harlacher et al. 2012), a three-component system taken from (Makaruk & Harasek 2009) and a multistage membrane system described in (Makaruk et al. 2010). In general, all the results were reproduced with good accuracy taking into account that our model does not incorporate a pressure drop and there were some uncertainties in the simulation parameters.

The absorption model was used to represent the results from pressurized water scrubbing in (Nock et al. 2014), chemical absorption of CO_2 with MEA in (Khan et al. 2011) and (Kasikamphaiboon et al. 2013) and chemical absorption of CO_2 with AMP in (Gabrielsen et al. 2006). The validation showed that the absorption column model applied provides results with an adequate agreement to the results presented in literature both in physical absorption and chemical absorption. There were some discrepancies in the concentration profiles along the column height, but the outlet concentrations were in a good agreement. Naturally the assumptions of constant temperature and pressure along the column height restricts the accuracy of the simulation results.

The simple energy consumption calculations produce the same order of energy consumption for the three processes as in (Ferreira et al. 2014). The comparison showed, however, that both the energy consumption of water scrubbing and chemical absorption are underestimated in our simulations.

3 Results and discussion

Two simulation campaigns following experimental designs were conducted. The first one incorporated selected process design and operational parameters. The second one tested the sensitivity of solver parameters. Matlab® was used to perform the simulations.

3.1 Process parameters

The aim of the experimental design and simulations was to demonstrate the sensitivity of some process parameters to the operation of different biogas purification processes. A biogas upgrading plant with a nominal feed flow of 1000 m^3/h and a target methane purity >95 % were assumed. A full factorial design (Diamond 1981) with two levels for five parameters was executed, producing a total amount of 32 experiments. The experimental design was applied for each of the three upgrading processes. The nominal simulation

parameters and the manipulated variables (MV) are listed in Table 1 and Table 2, respectively. For the absorption processes, the high levels for liquid flow rate and gas flow rate are 15 % higher than the nominal ones. For the chemical absorption, MEA concentration was altered instead of operation pressure. For the multistage membrane separation, membrane selectivity and area ratio were manipulated instead of operation temperature and liquid flow rate.

The output variables observed were biomethane production rate (PR), methane purity (MP) and specific energy consumption (SEC) with respect to treated biogas. In addition, a performance index presented in (Nock et al. 2014) was used:

$$PI = \frac{1 - \frac{y_{CH4}^{out}}{y_{CH4}^{in}}}{1 - \frac{y_{CH4}^{out}}{100}} \quad (10)$$

where y_{CH4}^{out} and y_{CH4}^{in} are gas molar fractions of CH4 in outlet and inlet, respectively.

Figures 1-3 show the most important findings in a boxplot graphs. In a boxplot graph, the red line inside the box represents the median value of the output variable (indicated in the y-axis) during the experiments with the level of the manipulated variable indicated in the x-axis. There is a statistically significant difference (with 95 % confidence) between the two levels of manipulated variable in the experimental design if notches around the two median values do not overlap.

For the water scrubbing (Figure 1), manipulated variables causing statistically significant changes in the output variables are feed flow rate, temperature and liquid flow rate. The increment in the liquid flow rate increases the specific energy consumption. This can be expected as more water requires more pumping. Decreasing the temperature has a positive effect on the performance index and methane purity. This phenomenon is due to higher solubility in low temperatures. Increasing the feed flow rate decreases the performance index and methane purity. However, it also decreases the specific energy consumption and naturally increases the production rate. The performance index and methane purity decrease since the increment in feed flow causes that the area of the mass transfer and the liquid flow with respect to the gas flow decrease. Among the tested manipulated variables, three combinations resulted in methane purity less than 95 %.

Table 1. Simulation parameters.

	WATER SCRUBBING	CHEMICAL ABSORPTION		MEMBRANE SEPARATION
Column/fiber height/length, L	11.0 m	8.1 m		0.38 m
Column/fiber diameter, d	1.06 m	0.355 m		0.000398 m
Gas flow, V_G	1000 m^3/h	1000 m^3/h		1000 m^3/h
CO_2 fraction, y_{CO2}	0.4	0.4		0.4
Liquid flow, V_L	145 m^3/h	7.8 m^3/h	**Number of fibers**	3000000
MEA/AMP concentration, $C_{L,i}$	n.a.	5000 mol/m^3	**Area ratio**	10
Operation temperature, T	25 °C	25 °C		25 °C
Operation pressure, P	9 bar	1 bar		10 bar
Final pressure	16 bar	16 bar		16 bar
Mass transfer coefficient of CO_2, K_{CO2}	0.0627 1/s	0.0627 1/s	**Permeance of CO_2, Q_{CO2}**	11.89 $mol/m^2/h/bar$
Mass transfer coefficient of CH_4, K_{CH4}	0.0609 1/s	n.a.	**Permeance of CH_4, Q_{CH4}**	0.24 $mol/m^2/h/bar$
Enhancement factor, E	1	150		n.a.
Compressor/pump efficiency	0.75	0.75		0.75
Discrete points, NoD	100	100		200
Relaxation factor, RF	0.4	0.05		0.4
Convergence criterion, CC	10^{-5}	10^{-9}		10^{-5}

Table 2. Manipulated variables in experimental design.

	WATER SCRUBBING	CHEMICAL ABSORPTION	MEMBRANE SEPARATION
MV1	Feed flow (m^3/h) 1=1000, 2=1150	Feed flow (m^3/h) 1=1000, 2=1150	Feed flow (m^3/h) 1=1000, 2=1150
MV2	CO_2 feed mole fraction 1=0.35, 2=0.40	CO_2 feed mole fraction 1=0.35, 2=0.40	CO_2 feed mole fraction 1=0.35, 2=0.40
MV3	Operation pressure 1=9 bar, 2=10 bar	MEA concentration 1=4.5, 2=5 $kmol/m^3$	Operation pressure 1=10 bar, 2=12 bar
MV4	Operation temperature 1=20 °C, 2=25 °C	Operation temperature 1=20 °C, 2=25 °C	Membrane selectivity 1=40, 2=50 (CO_2/CH_4)
MV5	Liquid flow (m^3/h) 1=145, 2=166.75	Liquid flow (m^3/h) 1=7.8, 2=8.97	Membrane area ratio 1=1, 2=10 (A2/A1)

DOI 10.3384/ecp1511955

In chemical absorption (see Figure 2), feed flow rate, CO_2 molar fraction and MEA concentration causes statistically significant changes to the output variables. The performance index decreases strongly by increasing the feed flow rate, but changes observed in the methane purity are less sensitive to the feed flow rate. Naturally the production rate is also affected by the feed flow rate. The CO_2 molar fraction has a strong effect on the specific energy consumption. This is due to the required reboiler duty that increases as the amount of CO_2 in the feed stream increases and more MEA need to be regenerated. The 15 % degradation in the MEA concentration has a similar effect on the performance index and methane purity than the 15 % increment in the feed flow rate. This can also be seen from the relative changes listed in Table 4. In chemical absorption, too low methane purity was observed in ten trials.

The membrane separation process shows sensitivity between the studied levels for operation pressure, feed flow rate and area ratio (Figure 3). Increasing the pressure increases the performance index and methane purity, increment in the feed flow rate increases the production rate and degradation of area ratio lowers the specific energy consumption considerably. The observations regarding operation pressure and feed flow rate are quite obvious. The last observation needs to be considered more closely. Increasing the area ratio while keeping the total membrane area constant means that the area of the first membrane decreases and the area of the second membrane increases. This leads to a situation where gas is mostly separated at the second stage. In the process structure used, permeate of the second stage is recycled to the first stage feed. Hence the total feed of the first stage membrane, as well as the amount of gas to be compressed into operation pressure, increases significantly. The results presented in (Makaruk et al. 2010) show the same effect, but also that the specific compression power only increases when the area ratio is higher than 1. For the area ratios less than one (i.e. first stage membrane area is larger than second stage), the compression power remains constant. Notice that in (Makaruk et al. 2010), the specific compression power is calculated with respect to produced gas. Here the calculation was made with respect to treated biogas. There were two experiments, where the required methane purity was not achieved.

When only the feed conditions are considered, i.e. the changes in feed flow rate and CO_2 feed fraction, the membrane separation shows no sensitivity (if the production rate is neglected). Based on these observations, membrane separation might be suitable for processes with a varying feed flow and CO_2 feed fraction. In chemical absorption, the CO_2 feed fraction has a strong effect on specific energy consumption. The performance index and methane purity decrease as the feed flow rate increases. The results suggest that chemical absorption would be recommended for processes with a homogeneous feed flow rate and CO_2 feed fraction. Water scrubbing shows no statistically significant sensitivity to the CO_2 feed fraction. Therefore it might be suitable for biogas feed with varying feed CO_2 content. The simulations however show that some combination of parameters results in methane purity under 95 %. The 15 % change in the feed flow rate is seen in all recorder parameters, but the performance index and methane purity remain at a tolerable level. For the higher feed flow, the variation in the results is considerably higher. The specific energy consumption decreases as the feed flow rate increases. However, the comparison of literature data and simulated energy consumption of water scrubbing suggested that the energy consumption is underestimated here.

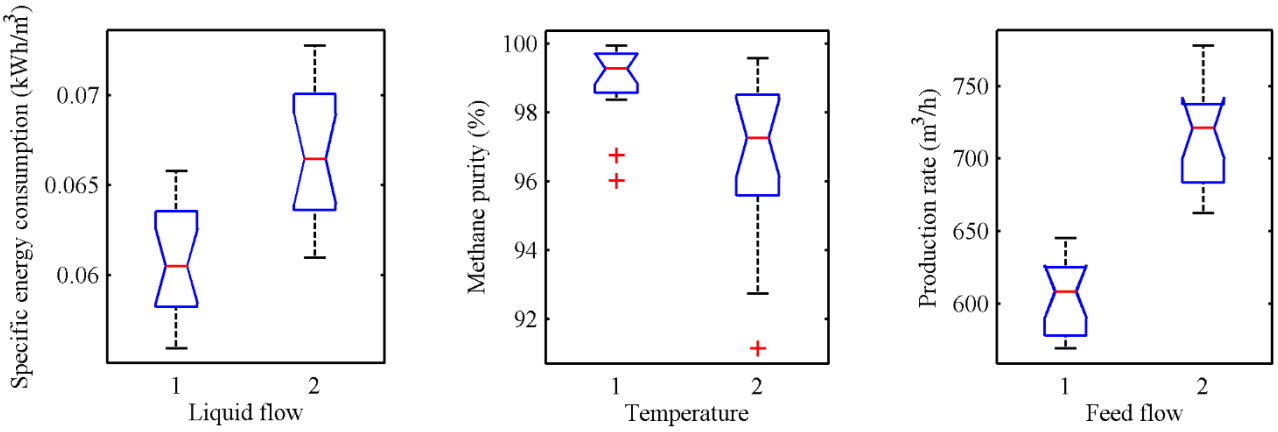

Figure 1. Selected boxplots from water scrubbing experiments.

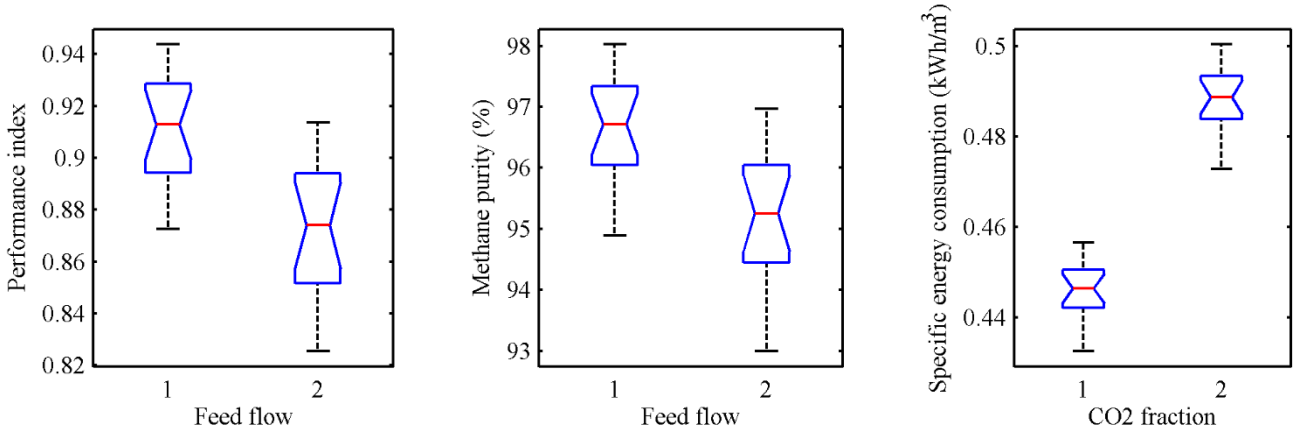

Figure 2. Selected boxplots from chemical absorption experiments.

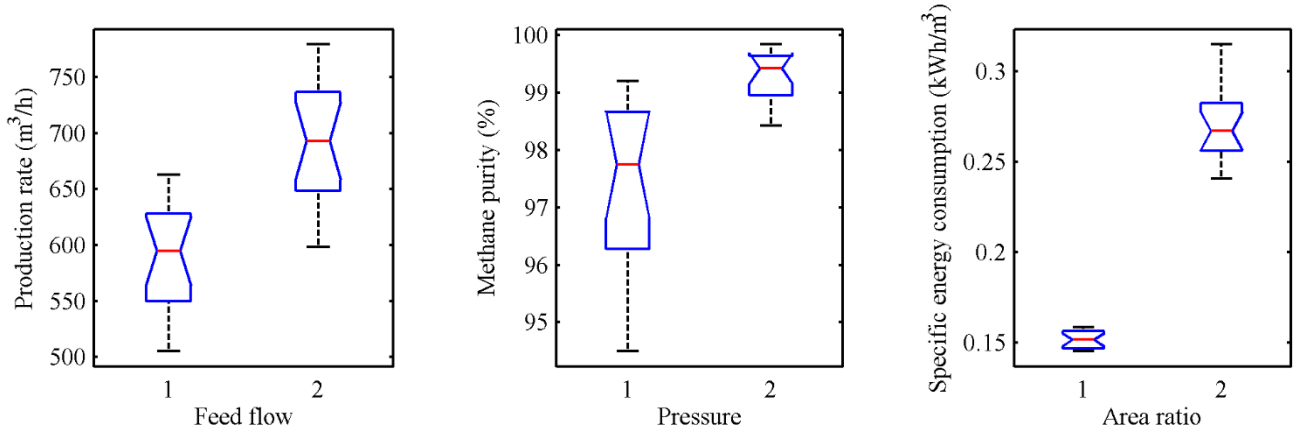

Figure 3. Selected boxplots from multistage membrane separation experiments.

Table 3. Manipulated solver parameter levels in experimental design.

	WATER SCRUBBING	CHEMICAL ABSORPTION	MEMBRANE SEPARATION
Number of discrete units (NoD)	1=75 2=100 3=150	1=75 2=100 3=150	1=150 2=200 3=300
Relaxation factor (RF)	1=0.3 2=0.4 3=0.5	1=0.04 2=0.05 3=0.06	1=0.3 2=0.4 3=0.5
Convergence criterion (CC)	1=5e-6 2=1e-5 3=5e-5	1=5e-10 2=1e-9 3=5e-9	1=5e-6 2=1e-5 3=5e-5

Table 4. Maximum relative change in the median during the experimental designs with respect to nominal results. The highlighted cells are the ones with statistically significant change.

		MV1	MV2	MV3	MV4	MV5	NoD	RF	CC
WS	**PI**	***9.1 %***	7.2 %	8.5 %	***9.2 %***	8.6 %	***0.5 %***	0 %	-0.1 %
	MP	***3.5 %***	2.9 %	3.3 %	***3.5 %***	3.3 %	***0.2 %***	0 %	-0 %
	PR	***20.1 %***	13.4 %	9.7 %	9.9 %	9.9 %	***0.2 %***	0 %	0 %
	SEC	***8.1 %***	4.6 %	5.9 %	3.7 %	***8.1 %***	***0.1 %***	0 %	0 %
CA	**PI**	***-4.2 %***	-2.4 %	***-4.1 %***	-3.8 %	-2.0 %	0 %	***-7.3 %***	0 %
	MP	***-1.3 %***	-0.9 %	***-1.2 %***	-1.1 %	0.4 %	0 %	***-2.8 %***	0 %
	PR	***21.6 %***	16.5 %	13.1 %	13.0 %	12.1 %	0 %	***2.8 %***	0 %
	SEC	-6.6 %	***-9.6 %***	-6.6 %	-6.5 %	-5.9 %	0 %	***-3.2 %***	0 %
MS	**PI**	2.7 %	2.2 %	***3.2 %***	2.2 %	2.4 %	***-0.1 %***	0.2 %	0 %
	MP	2.2 %	1.7 %	***2.4 %***	1.8 %	2.3 %	***-0.1 %***	0 %	0 %
	PR	***13.0 %***	7.8 %	6.1 %	5.0 %	10.4 %	***0.1 %***	-0 %	0 %
	SEC	-27.1 %	-27.1 %	-27.7 %	-27.5	***-44.7 %***	***0.1 %***	0.1 %	0 %

DOI
10.3384/ecp1511955

3.2 Solver parameters

The sensitivity of the results to the solver parameters was also tested. A full factorial design with three levels for the three adjustable parameters was simulated. The parameter levels are presented in Table 3. In Table 4, the results from both the process parameter experiments and the solver parameter experiments are listed as a maximum relative change in the median during the simulations. The results presented in Table 4 show that the relative changes in the observed output variables due to changes in the solver parameters are considerably lower with respect to changes caused by the manipulation of process parameters. The only exception is the relaxation factor in chemical absorption. These results suggest that the numerical algorithm is applicable to solving these type of problems once suitable solver parameters are found. The optimization of the solver parameters might only be necessary if the minimization of the CPU time is of interest.

4 Conclusions

Three potential CO_2 separation processes for biogas purification were modelled. Model parameters were scaled for 1000 m^3/h biogas treatment and simulation campaign following an experimental design was conducted in order to see the sensitivity of the process behavior for some process disturbances and design parameters. The results show that the 15 % increment in the feed flow rate does not solely produce intolerable methane purity (<95 %) in any of the processes, indicating that each process retain some level of controllability. Multistage membrane separation and pressurized water scrubbing seem preferable for processes with varying biogas feed flow and CO_2 feed fraction. On the opposite, chemical absorption with MEA show more sensitivity to those parameters and is therefore more suitable for processes with rather constant feed conditions. The performance of the numerical algorithm was found to be good as the results did not show intolerable sensitivity to the parameters of the numerical algorithm.

Acknowledgements

This research was conducted during SmartH_2/CH_4-Oulu research project. ERDF(EAKR) and TEKES are gratefully thanked for enabling the project.

References

Diamond, W. *Practical experimental designs for engineers and scientists*, Van Nostrand Reinhold, New York, 1981, 0-534-97992-0.

Ferreira A., Ribeiro A., Kulaç S., Rodrigues A. (2014) Methane purification by adsorptive processes in MIL-53(Al), *Chemical Engineering Science*, 124, 79-95. doi:10.1016/j.ces.2014.06.014.

Gabrielsen J., Michelsen M., Stenby E., Kontogeorgis G. (2006) Modeling of CO2 absorber using an AMP solution, *AIChE Journal*, 52(10), 3443-3451. doi:10.1002/aic.10963.

Greer T. 2008, *Modeling and simulation of post combustion CO2 capturing*, M.Sc thesis, Telemark University College, Porsgrunn, Norway.

Hall S. (2012) *Branan's rules of thumb for chemical engineers*, 5th ed., Butterworth-Heinemann 2012, 978-0-12-387785-7.

Harlacher T., Scholz M., Melin T., Wessling M. (2012) Optimizing argon recovery: membrane separation of carbon monoxide at high concentrations via the water gas shift, *Industrial & Engineering Chemistry Research*, 51(38), 12463-12470. doi:10.1021/ie301485q.

Kasikamphaiboon P., Chungsiriporn J., Bunyakan C., Wiyaratn W. (2013) Simulataneous removal of CO2 and H2S using MEA solution in a packed bed column absorber for biogas upgrading, *Songklanakarin Journal of Science and Technology*, 35(6), 683-591.

Khan F.M., Krishnamoorthi V., Mahmud T. (2011) Modelling reactive absorption of CO2 in packed columns for post-combustion carbon capture applications, *Chemical Engineering Research and Design*, 89(9), 1600-1608. doi:10.1016/j.cherd.2010.09.020.

Kucka L., Müller I., Kenig E.Y., Górak A. (2003) On the modelling and simulation of sour gas absorption by aqueous amine solutions, *Chemical Engineering Science*, 58(16), 3571-3578. doi:10.1016/S0009-2509(03)00255-0.

Makaruk A., Harasek M., (2009) Numerical algorithm for modelling multicomponent multipermeator systems, *Journal of Membrane Science*, 344, 258-265. doi:10.1016/j.memsci.2009.08.013.

Makaruk A., Miltner M., Harasek M. (2010) Membrane biogas upgrading processes for the production of natural gas substitute, *Separation and Purification Technology*, 74(1), 83-92. doi:10.1016/j.seppur.2010.05.010.

Mohebbi V., Naderifar A., Behbahani R.M., Moshfeghian M. (2012) Determination of Henry's law constant of light hydrocarbon gases at low temperatures, *The Journal of Chemical Thermodynamics*, 51, 8-11. doi:10.1016/j.jct.2012.02.014.

Nock W., Walker M., Kapoor R., Heaven S. (2014) Modeling the Water Scrubbing Process and Energy Requirements for CO2 Capture to Upgrade Biogas to Biomethane, *Industrial & Engineering Chemictry Research*, 53(32), 12783-12792. doi: 10.1021/ie501280p.

Scholz M. (2013) *Membrane based biogas upgrading processes*, Ph.D. dissertation, RWTH Aachen University, 2013.

Wellinger A., Murphy J., Baxter D. (eds.) *The Biogas Handbook: Science, Production and Applications*, Woodhead Publishing Limited 2013, 978-0-85709-498-8.